Therapeutic Silencing of miR-214 Inhibits Tumor Progression in Multiple Mouse Models

Molecular Therapy
Original Article

Therapeutic Silencing of miR-214 Inhibits Tumor Progression in Multiple Mouse Models

Daniela Dettori,[1,2,6] Francesca Orso,[1,2,3,6] Elisa Penna,[1,2,6] Désirée Baruffaldi,[1,2] Serena Brundu,[4,5] Federica Maione,[4,5] Emilia Turco,[1,2] Enrico Giraudo,[4,5] and Daniela Taverna[1,2,3]

[1]Molecular Biotechnology Center (MBC), University of Torino, Torino, Italy; [2]Department Molecular Biotechnology and Health Sciences, University of Torino, Torino, Italy; [3]Center for Complex Systems in Molecular Biology and Medicine, University of Torino, Torino, Italy; [4]Department of Science and Drug Technology, University of Torino, Torino, Italy; [5]Candiolo Cancer Institute, FPO-IRCCS, 10060 Candiolo, Torino, Italy

We previously demonstrated that miR-214 is upregulated in malignant melanomas and triple-negative breast tumors and promotes metastatic dissemination by affecting a complex pathway including the anti-metastatic miR-148b. Importantly, tumor dissemination could be reduced by blocking miR-214 function or increasing miR-148b expression or by simultaneous interventions. Based on this evidence, with the intent to explore the role of miR-214 as a target for therapy, we evaluated the capability of new chemically modified anti-miR-214, R97/R98, to inhibit miR-214 coordinated metastatic traits. Relevantly, when melanoma or breast cancer cells were transfected with R97/R98, anti-miR-214 reduced miR-214 expression and impaired transendothelial migration were observed. Noteworthy, when the same cells were injected in the tail vein of mice, cell extravasation and metastatic nodule formation in lungs were strongly reduced. Thus, suggesting that R97/R98 anti-miR-214 oligonucleotides were able to inhibit tumor cell escaping through the endothelium. More importantly, when R97/R98 anti-miR-214 compounds were systemically delivered to mice carrying melanomas or breast or neuroendocrine pancreatic cancers, a reduced number of circulating tumor cells and lung or lymph node metastasis formation were detected. Similar results were also obtained when AAV8-miR-214 sponges were used in neuroendocrine pancreatic tumors. Based on this evidence, we propose miR-214 as a promising target for anti-metastatic therapies.

INTRODUCTION

The ability of tumors to spread in their host organism is a main issue in cancer treatment, as metastasis formation accounts for more than 90% of human cancer deaths. Tumor progression depends on alterations of transformed cells and reprogramming of the surrounding microenvironment, which culminates with the escaping of malignant cells from the primary mass to distant organs.[1] Melanomas, pancreatic tumors, and some subtypes of breast cancers are highly invasive and too often fatal diseases.[2] Several studies report the relevance of microRNAs (miRs) during the metastatic process of these neoplasias and suggest a possible miR-based therapeutic intervention.[3] We and others recently observed that miR-214 is strongly expressed in malignant melanomas versus *in situ*, non-disseminated transformed melanocytic growths, in triple-negative breast cancers as well as in different pancreatic tumors and unraveled its pro-metastatic functions.[4–15] Our studies also demonstrated that miR-214 controls dissemination by acting on a large number of direct and indirect targets, among them regulators of transcription such as TFAP2, adhesion molecules, i.e., ITGA5 and ALCAM, as well as other miRs, in particular miR-148b, a small RNA with anti-metastatic functions. More recently, we explored the relevance of miR-214 and miR-148b for miR-based targeted therapies and analyzed the dissemination of miR-214 sponge-depleted and miR148b-overexpressing cells in mice. Relevantly, we demonstrated that single or combined modulations of miR-214 (inhibition) and miR-148b (overexpression) in tumor cells could inhibit metastatization by blocking extravasation, consequent to the decrease of ITGA5 and ALCAM, respectively involved in tumor-extracellular matrix (ECM) and tumor-endothelial cell interactions.[15] Several papers show that it is possible to inhibit the function of miRs pharmacologically with complementary chemically modified oligonucleotides, called anti-miRs or antagomiRs.[16,17] Anti-miRs are short oligonucleotides complementary to target miRs containing chemical modifications to optimize base pairing and increase resistance to nucleases with optimal pharmacokinetic properties.[18] Up to now, a successful anti-miR clinical intervention has been obtained using anti-miR-122 in patients with chronic hepatitis C virus (HCV) infection. Here, a substantial viral load reduction has been observed 4 weeks after the injection of a subcutaneous single dose of the modified anti-miR-122 RG-101.[19] In addition, a clinical intervention for patients with Alport syndrome, a life-threatening genetic kidney disease with no approved therapies, is currently ongoing with an anti-miR-21.[20,21] Considering the

Received 18 December 2017; accepted 21 May 2018;
https://doi.org/10.1016/j.ymthe.2018.05.020.

[6]These authors contributed equally to this work.

Correspondence: Daniela Taverna, MBC and Department Molecular Biotechnology and Health Sciences, University of Torino, Via Nizza, 52, 10126 Torino, Italy.
E-mail: daniela.taverna@unito.it
Correspondence: Francesca Orso, MBC and Department Molecular Biotechnology and Health Sciences, University of Torino, Via Nizza, 52, 10126 Torino, Italy.
E-mail: francesca.orso@unito.it

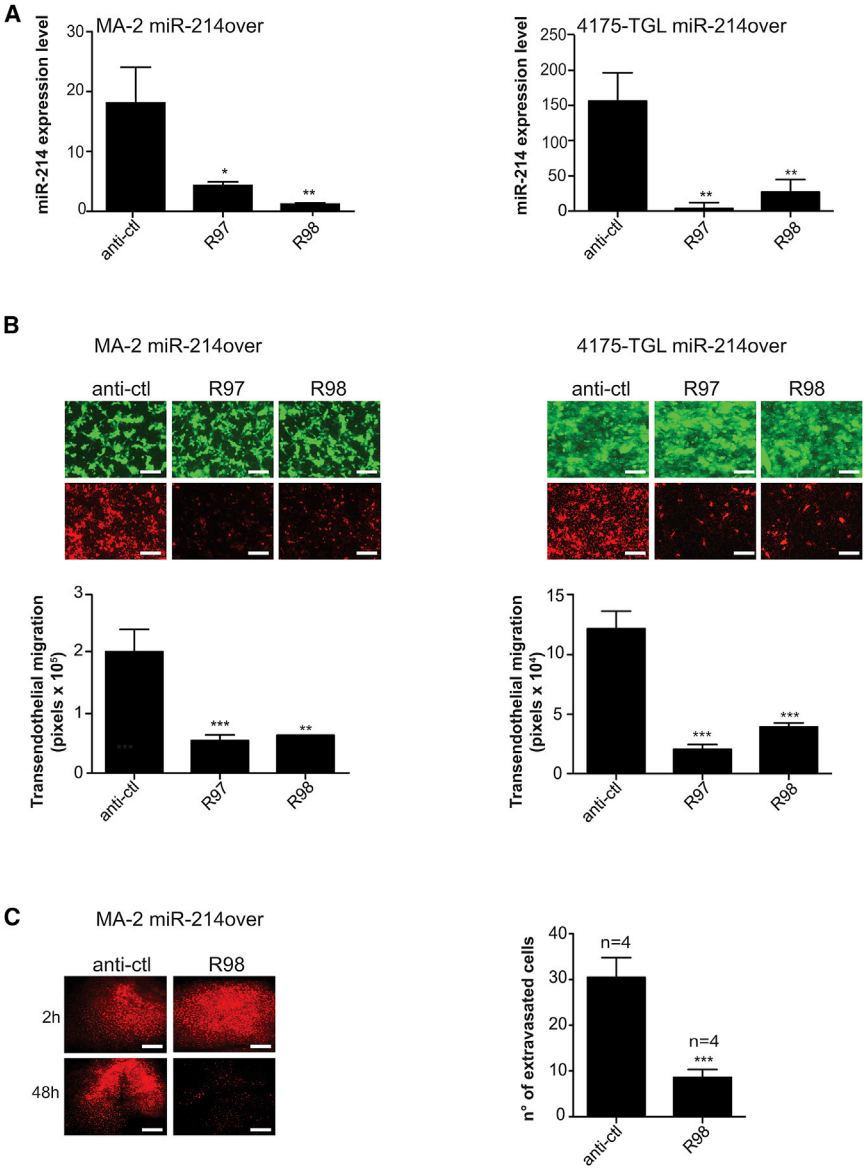

Figure 1. R97 and R98 anti-miR-214 Suppress miR-214 Expression in Melanoma and Breast Cancer Cells and Inhibit Transendothelial Migration and Extravasation

(A) miR-214 expression levels in tRFP-expressing MA-2 and 4175-TGL miR-214over cells transiently transfected with R97 or R98 anti-miR-214 or anti-miR controls (anti-ctl), for 48 hr, measured by qRT-PCR analysis presented as fold changes (mean ± SD of triplicates) relative to the median of miR-214 expression, normalized on U6 RNA. (B) Transendothelial migration through a HUVEC monolayer on top of a porous membrane was evaluated for MA-2 and 4175-TGL miR-214over cells transfected as in (A). Results are expressed as mean ± SEM of the area covered by migrated cells. Representative pictures of the HUVEC monolayer (GFP) and transmigrated cells (tRFP) are shown. (C) *In vivo* extravasation 2 hr or 48 hr following tail-vein injections in immunodeficient mice of CMRA-labeled tRFP-expressing MA-2-miR-214over cells transiently transfected with R98 anti-miR-214 or anti-miR controls (anti-ctl). The graph (right) shows the number of extravasated cells as mean ± SEM at 48 hr for the indicated number (n) of mice. Representative pictures of whole fluorescent lungs at 2 hr (lung lodging) or 48 hr post-injection are shown; scale bars, 1 mm. For all assays, at least two independent experiments were performed (with triplicates for *in vitro* studies) and representative results are shown. *$p < 0.05$; **$p < 0.01$; ***$p < 0.001$.

relevant expression of miR-214 in malignant melanoma, breast, and pancreatic tumors,[4–15] we investigated the capability of R97 or R98 anti-miR-214 or AAV8-miR-214 sponge to block the dissemination of those primary tumors in mice following systemic administrations of the compounds.

RESULTS

Anti-miR-214 Reduces miR-214 Levels and Impairs Metastatic Traits of miR-214 Overexpressing Melanoma and Triple-Negative Breast Cancer Cells

Malignant melanomas and triple-negative breast cancers express high levels of miR-214, a small RNA with a proven pro-metastatic function as in Penna et al.[4] Here, we used MA-2 melanoma and 4175-TGL breast cancer cells overexpressing (over) miR-214 and turbo red fluorescent protein (tRFP)[4,15] to evaluate the relevance of miR-214 as therapeutic target. When MA-2 and 4175-TGL miR-214over cells were transfected with a modified R97 or R98 anti-miR-214 compound[22] and compared to cells transfected with a generic anti-miR control (anti-ctl), miR-214 expression was strongly inhibited for both cell lines, as measured by qRT-PCR analysis (Figure 1A). In addition, migration through a porous membrane (transwell assay) or transendothelial migration through a Human Umbilical Vein Endothelial cell (HUVEC) monolayer was strongly reduced (Figures S1 and 1B). More importantly, when R98-transfected cells were injected in the tail vein of immunosuppressed mice (n = 4), *in vivo* extravasation was strongly impaired compared to controls (n = 4), as evaluated 48 hr post-injection (Figure 1C). However, at 2 hr post-injection, no difference in lodging was observed between control and experimental cells, suggesting that both cell populations equally reached the lung capillaries in this time frame (Figure 1C). Relevantly, when R97 or R98 anti-miR-214-transfected cells were used to evaluate metastatic formation *in vivo* 3 weeks post-injection (tail vein), a strong reduction in nodule formation was observed for both MA-2 and 4175-TGL miR-214over-transfected cells compared to controls, as shown in Figures 2A and 2B. Taking all these results together, we can conclude that R97 or R98 anti-miR-214 compounds are

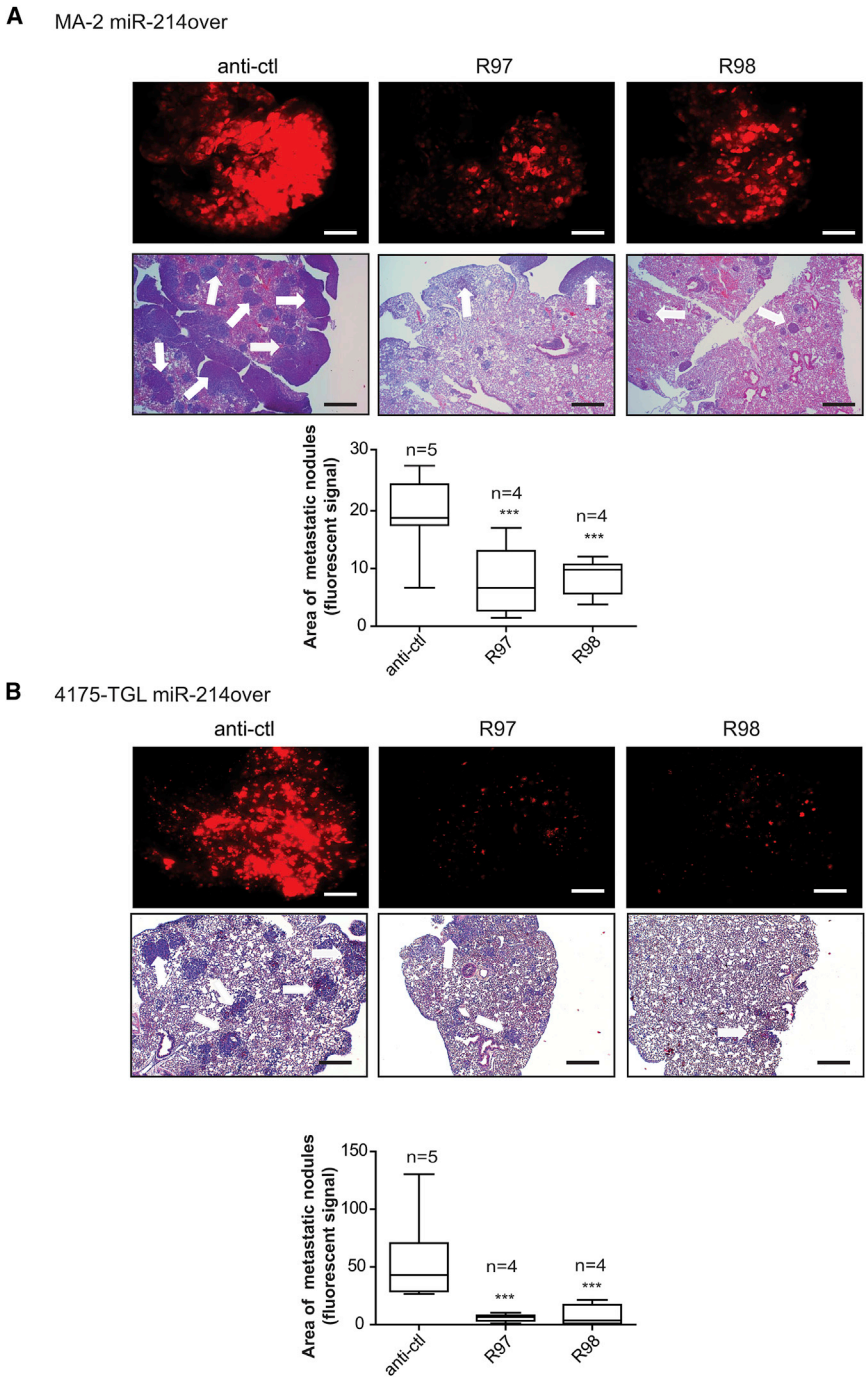

Figure 2. R97 or R98 anti-miR-214 Inhibit Lung Metastatic Nodule Formations of Melanoma and Breast Cancer Cells

Lung colony formation in immunodeficient mice, 3 weeks after tail-vein injection of tRFP-expressing MA-2 (A) or 4175-TGL (B) miR-214over cells transiently transfected with R97 or R98 anti-miR-214 or anti-miR controls (anti-ctl). Graphs (bottom of each figure) represent quantitated results as mean ± SEM of metastatic fluorescent areas in lungs, referring to the indicated number (n) of mice. Representative pictures of fluorescent whole lungs (scale bars, 1 mm) and H&E-stained sections (scale bars, 100 μm) are shown. Two independent experiments were performed, and a representative one is shown. ***$p < 0.001$.

promising in the control of miR-214 expression and miR-214-dependent dissemination.

Systemic Treatments of Mice Carrying Melanoma or Breast Cancer Primary Tumors with Anti-miR-214 Impair Metastasis Formation

To evaluate primary tumor formation and metastatic dissemination *in vivo*, tRFP-expressing MA-2 and 4175-TGL miR-214over cells were injected, respectively, subcutaneously (n = 12 versus n = 11 mice) or in the mammary gland fat pad (n = 18 versus n = 11 mice). Tumor growth and metastatic dissemination to the lungs were evaluated 37 or 25 days later, respectively, in mice treated with R98 anti-miR-214 (0.25 mg/mouse in 200 μL of PBS) or with the same volume of PBS, used as control, every other day until mice were sacrificed (Figures 3A and 3B). The measurement of the primary tumor mass expressed as weight in grams, revealed no difference between R98-treated or control mice for both cell lines (Figures 3C and 3D). However, metastatic dissemination from primary tumors to the lungs, measured as number or area of fluorescent metastasis in whole lungs and as total cell or colony number of plated circulating tumor cells (CTCs), resulted strongly reduced in R98-treated versus control mice (Figures 3E–3H) for both cell lines. Relevantly, R98 led to reduced miR-214 expression in primary MA-2 and 4175-TGL miR-214over-derived tumors (n = 5 or 6) compared to controls (n = 5 or 6) as in (Figures 3I and 3J). For 4175-TGL miR-214over-derived tumors, we also observed increased levels of miR-148b, a miR-214 downstream player, and decreased expression of two of its direct targets, the adhesion molecules *ALCAM* and *ITGA5* that we previously found involved in the control of extravasation (Figure S2). MA-2 miR-214 over-derived tumors did not show similar modulations (data not shown), suggesting the possibility of additional mechanisms in melanomas. In summary, we can conclude that R97 or R98 anti-miR-214 compounds are powerful therapeutic tools able to control metastatic dissemination from primary melanoma and breast cancer tumors.

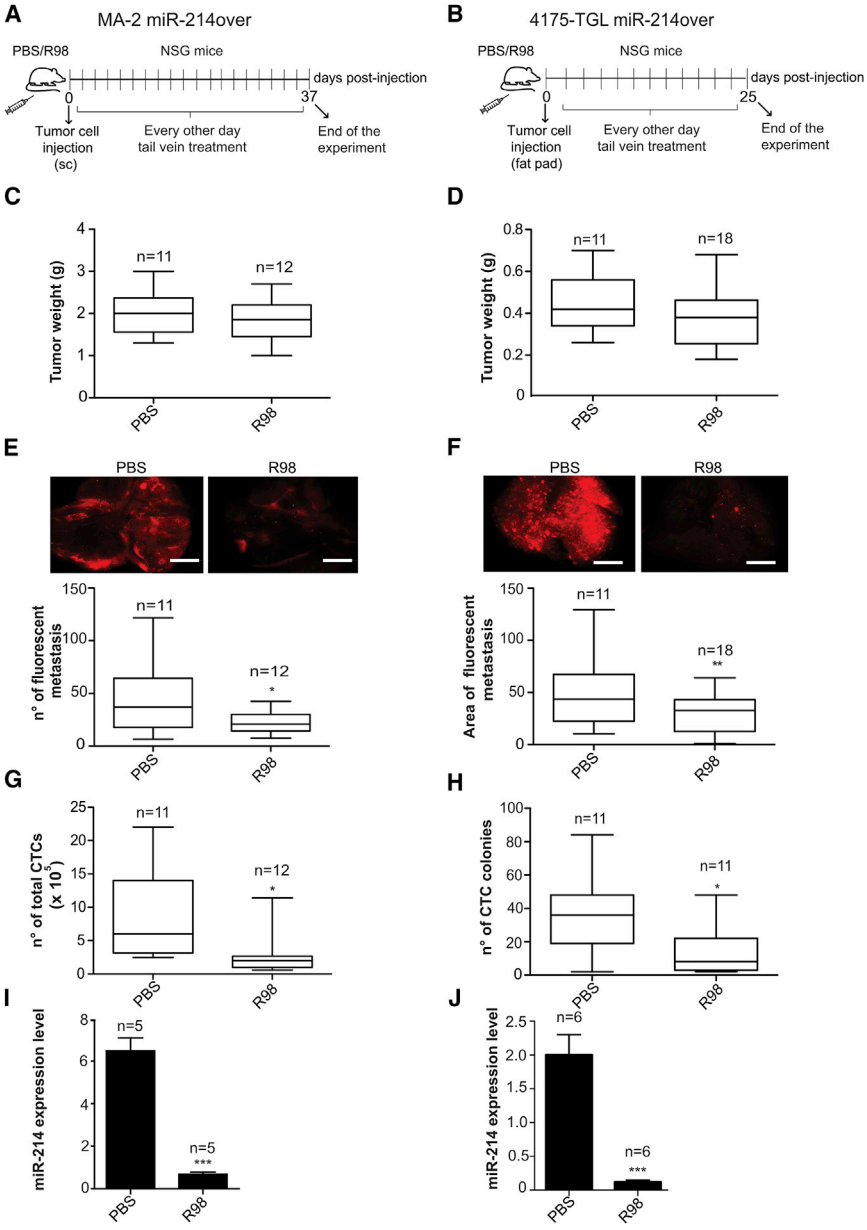

Figure 3. Systemic Treatments of Mice Bearing Primary Melanoma or Breast Cancer Tumors with R98 anti-miR-214 Impair Metastasis Formation

Schemes summarizing the protocols used to treat the animals (A and B). tRFP-expressing MA-2 (A, C, E, G, and I) or 4175-TGL (B, D, F, H, and J) miR-214over cells were injected, respectively, subcutaneously or in the mammary gland fat pad, and mice were systemically treated with 0.25 mg/mouse of R98 anti-miR-214 (in 200 μL PBS) or PBS only (same volume), with tail-vein injections, the day after cell inoculation and every other day until the end of the experiment. Mice were sacrificed 37 (A) or 25 (B) days post-injection and primary tumor weight for MA-2 (C) and 4175_TGL miR-214over cell (D), lung metastasis formations for MA-2 (E), and 4175-TGL miR-214over cell (F) and circulating tumor cells (CTCs) for MA-2 (G) and 4175-TGL miR-214over cell were evaluated for the indicated number (n) of mice. Expression of miR-214 was evaluated in MA-2 (I) and 4175-TGL (J) miR-214over cell-derived primary tumors by qRT-PCR analysis and presented as fold changes (mean ± SD of triplicates) relative to median of miR expression, normalized on U6 RNA in n = 5 or 6 mice per group. Tumor weight, mean ± SEM of grams; metastasis, mean ± SEM of number or area of fluorescent metastases; CTCs, mean ± SEM of number of total or derived colonies of circulating tumor cells grown in plates from blood samples at the end point of the experiments. Representative pictures of fluorescent whole lungs (scale bars, 1 mm) are shown (E and F). sc, subcutaneous. *$p < 0.05$; **$p < 0.01$; ***$p < 0.001$.

Anti-miR-214 or AAV8-miR-214 Sponge Administration Impairs Tumor Growth and Local Metastatization in the RIP-Tag2 spontaneous Mouse Model of Pancreatic Neuroendocrine Cancer

In order to evaluate the therapeutic potential of anti-miR-214-based treatments on the dissemination of spontaneous carcinogenesis, miR-214 activity was inhibited in the RIP-Tag2 mouse model of pancreatic neuroendocrine tumor, a neoplasia where miR-214 expression is associated with the tumor angiogenic switch.[5] As shown in Figure 4, intraperitoneal treatment (twice a week from week 12 to 16) of n = 8 mice with R97 or R98 anti-miR-214 (0.25 mg/mouse in 200 μL of PBS) led to reduced tumor volume when compared to n = 7 PBS-injected mice (Figures 4A and 4B). Notably, a dramatic decrease of peripancreatic lymph node (LN) metastasis volume was observed in R97- or R98-treated mice compared to controls (Figure 4C) as shown by SV40 T antigen (TAg) immunostaining (Figure 4C, arrows). When miR-214 expression was evaluated in sections of whole pancreas containing neuroendocrine islets, a significant decrease was observed in R97- or R98-treated mice (n = 6) compared to controls (n = 5), while miR-148b remained unaltered (Figure S3A). Similarly to R97- or R98-treated mice, when a group of n = 8 RIP-Tag2 mice was treated with adeno-associated viruses-serotype 8 expressing miR-214 sponge (AAV8-miR-214 sponge, one mesenteric artery injection, at week 12) and compared to n = 8 PBS-injected controls (Figure 4D), tumor volume was also reduced (Figure 4E) and local mestastatization into the peripancreatic LNs was strikingly decreased (Figure 4F). Interestingly, by performing MECA32 immunostaining, a statistically significant decrease in vessel areas (Figure 4G) was observed on primary tumor masses grown in R97 or R98 or AAV8-miR-214 sponge-treated animals (n = 5), which could explain in part the decreased tumor growth. Besides reduced vascularization, a diminished rate of proliferation (measured by Ki67 immunostaining) was observed in primary

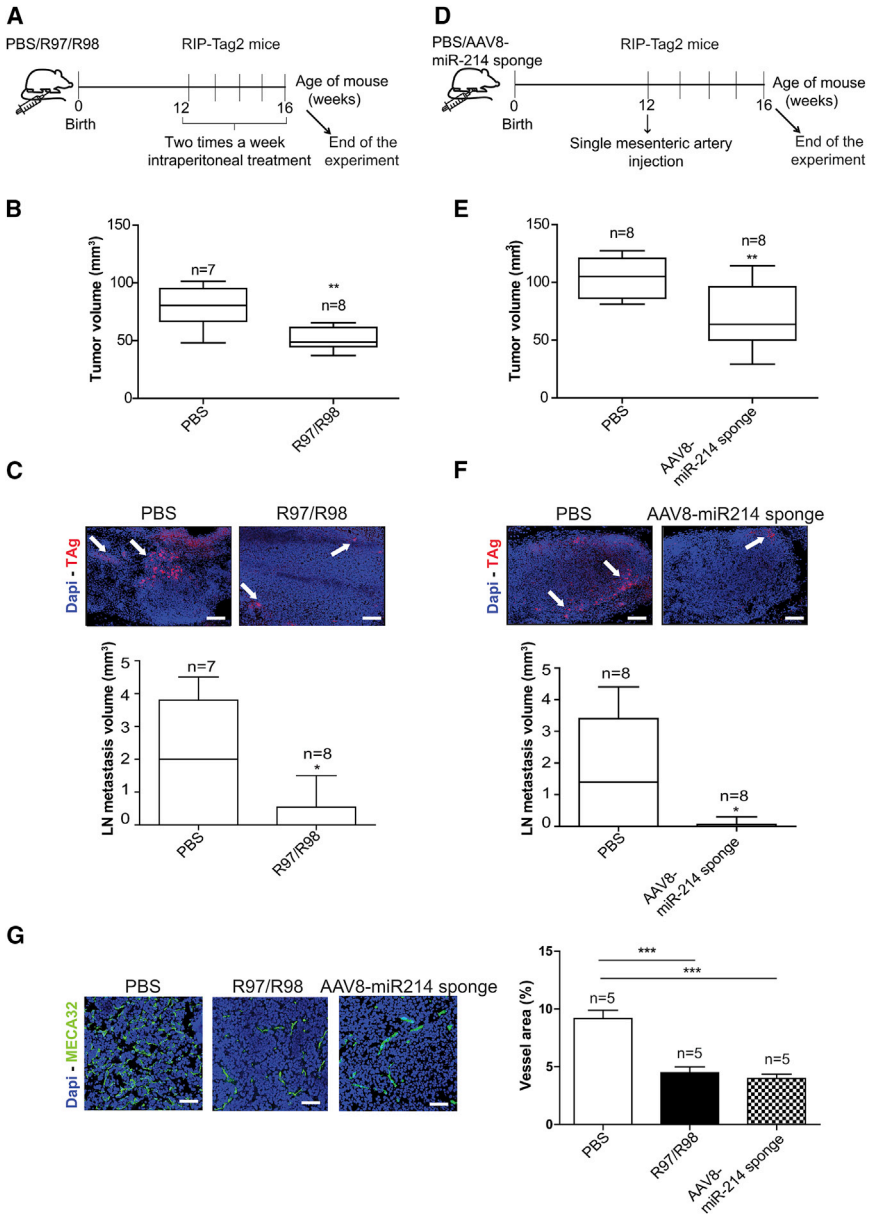

Figure 4. R97 or R98 Anti-miR-214 or AAV8-miR-214 Sponge Administration Suppresses Tumor Growth and Impairs Local Metastatization to Local Lymph Nodes in a Spontaneous Model of Pancreatic Neuroendocrine Cancer (RIP-Tag2)

RIP-Tag2 mice were treated twice a week for 4 weeks (from weeks 12 to 16) with R97/R98 anti-miR-214 (A) intraperitoneally, or once at week 12, with AAV8-miR-214 sponge (D) via injections in the mesenteric artery; PBS was administered in negative control animals. All mice were sacrificed at week 16 for tumor and metastasis evaluations. Tumor growth (B and E) was analyzed by measuring tumor volume (mm^3) for R97/R98 anti-miR-214- (B) and AAV8-miR-214 sponge (E)-treated mice. Instead, local metastatization in peripancreatic lymph nodes (LNs) for R97/R98 anti-miR-214- (C) and AAV8-miR-214 sponge (F)-treated mice was evaluated by SV40 T antigen immunostaining (TAg, arrows) while DAPI was used to stain nuclei. Representative images were derived from serial section analysis of LNs in each animal (scale bars, 50 μm). (G) Vascularization of the primary tumors (referring to B and E) was evaluated by MECA32 immunostaining while DAPI was used to stain nuclei. Representative images are shown (scale bars, 50 μm). Mean ± SEM of tumor volume (mm^3) or LN metastasis volume (mm^3) or areas occupied by capillaries versus total area (percentage, %) are shown for the indicated number (n) of mice in the graphs. *$p < 0.05$; **$p < 0.01$; ***$p < 0.001$.

tumors of R97- or R98-injected animals, while no alteration in apoptosis (measured by cleaved caspase 3 immunostaining) was detected here (Figure S3B). All these results together led us to conclude that miR-214 inhibition is a powerful strategy to reduce neuroendocrine pancreatic growth and metastatization, giving hope for a transfer to the clinics.

Anti-miR-214 or AAV8-miR-214 Sponge Administration Does Not Show Signs of Toxicity in Mice

In order to evaluate R97/R98 anti-miR-214 toxicity in both immunocompetent or immunosuppressed animals, these compounds or PBS (used as control) were delivered to tumor-free C57/Bl6 or NOD/SCID/IL2R_null (NSG) (mixed background) mice every other day, for 1 month, by tail-vein injections. The potential toxicity of AAV8-miR-214 sponges was assessed in C57/Bl6 mice by weekly intraperitoneal treatments, for 1 month. For all experiments, normalized body and organ (liver, spleen, and kidneys) weights were evaluated after 1, 2, 3, and 4 weeks of treatment (as indicated) or at the end of the experiments only (Figures 5A–5C, 6A, and 6B), for the indicated number of animals (n) per group. In addition, organ histology was analyzed on H&E-stained sections (Figures 5C, 6A, and 6B). Expression of specific markers described to be associated with toxicity, such as *p56*, *OAS1*, *IL-6*, and *IL-8*[23] was also evaluated in liver (Figures 7A–7D), spleen (Figures S4A–S4D), and kidneys (Figures S5A–S5D) of treated versus control animals. Since no differences were observed for all studies (Figures 5, 6, 7, S4, and S5), we conclude that the compounds are not toxic for the animals, at least based on the protocols of treatment we applied.

DISCUSSION

The inability to fight metastasis formation remains the major failure of the clinicians in the cure of neoplasia. New and target-specific molecules to fight cancer have been developed also in conjunction with molecules with immunotherapeutic values. However, next to an initial

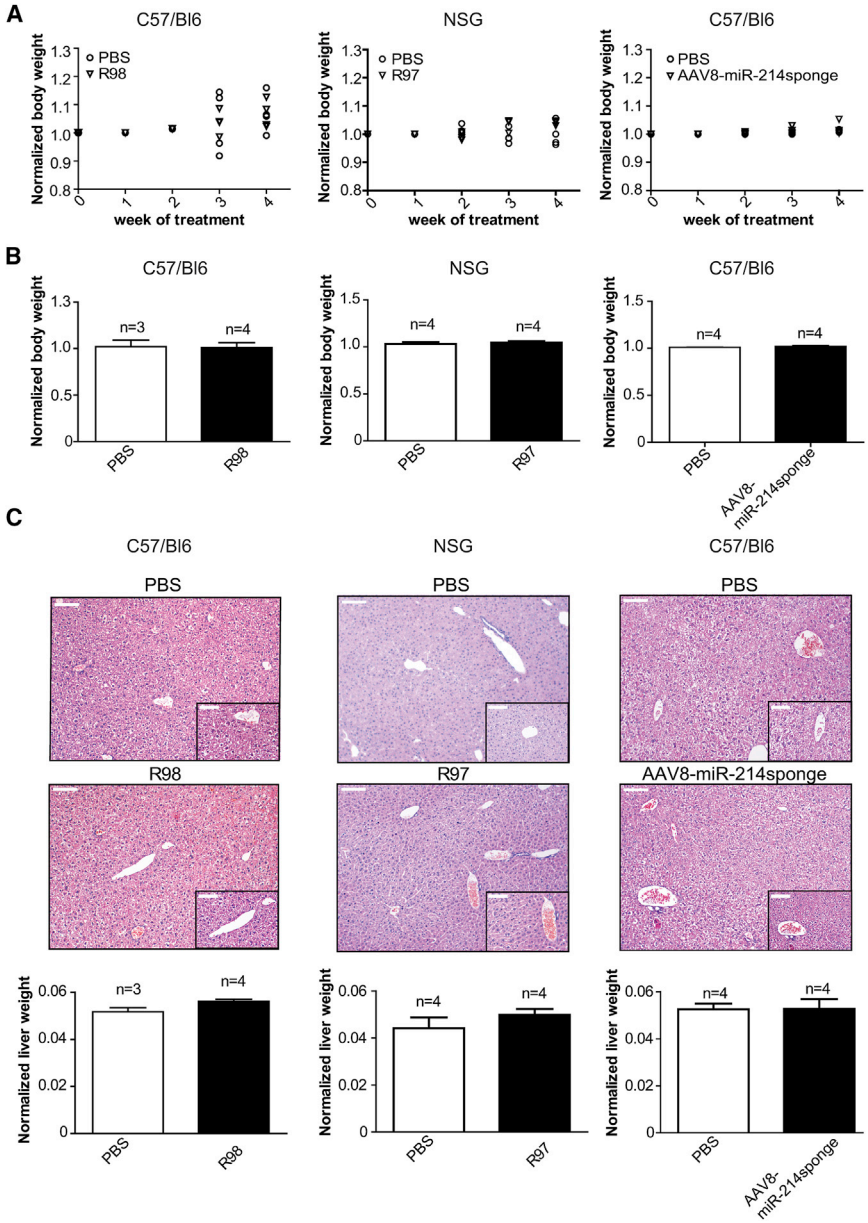

Figure 5. R97 or R98 anti-miR-214 or AAV8-miR-214 Sponge Administration Does Not Alter Animal Body Mass or Liver Weight and Histology

(A–C) Tumor-free immunocompetent C57/Bl6 or immunosuppressed NSG (mixed background) animals were weighted (g) and tail vein injected with R97/R98 anti-miR-214 compounds every other day for 1 month. Alternatively, animals were injected weekly intraperitoneally with AAV8-miR-214 sponges for 1 month. PBS was used as control for all experiments. (A and B) Body weight was measured during the experiment at the end of weeks 1, 2, 3, and 4 (final time) and presented as the normalized body weight (final weight subtracted from the initial value) of every mouse at each time point (A) or as mean ± SEM of the normalized body weight at final time (B). (C) For the same treated mice, representative pictures of H&E-stained liver sections (scale bars, 100 μm) are also shown. In addition, liver weight was evaluated at week 4 post-treatment, and it is plotted here as mean ± SEM of normalized liver weight (organ weight versus initial mouse body weight). n, number of mice used.

success, most of the molecular therapies failed because of insurgent tumor cell resistance. The development of new therapies is therefore essential. miR-based therapies have emerged as promising modern tools to fight cancer, in particular when surgery and standard interventions fail. In this paper, we propose the therapeutic application of small modified and stabilized anti-miR-214 (R97 or R98) to block the dissemination of malignant melanomas, triple-negative breast cancers, and neuroendocrine pancreatic tumors, three malignant cancers with relevant expression of miR-214. We also propose to use AAV8-miR-214 sponge to specifically treat neuroendocrine pancreatic tumors in RIP-Tag2 mice due to AAV8 distinct tropism. We provide evidence that the targeting of miR-214 in tumor cells, by transient transfections, leads to malignancy suppression (evaluated as nodule formation in lungs) mostly by inhibiting cell movement per se or through the endothelium monolayer, as shown by *in vitro* transwell migration assays and by transendothelial migration using HUVECs, as well as by extravasation experiments in mice, similar to other approaches we used previously.[4] More importantly, we show that when mice bearing miR-214-rich xenotransplants derived from malignant melanomas or breast cancers, or endogenous pancreatic neuroendocrine tumors (RIP-Tag2 model), were treated either systemically (tail vein, mice with xenotransplants) or intraperitoneally (RIP-Tag2 mice), with R97 or R98 anti-miR-214 compounds, metastatization to the lungs or to the local lymph nodes and circulation of tumor cells were strongly impaired, giving hope for a transfer to the clinics for anti-miR-214 tools. Thus, implying that, as shown previously, modified anti-miRs must have relevant tissue bioavailability, mostly assisted by plasma protein binding that reduces glomerular filtration, urinary excretion, and stability due to oligo modifications.[24] Considering that systemic administration of anti-miR-214 oligos does not lead to specific delivery, and therefore miR-214 silencing occurs for all cells expressing it, tumor and normal tissues, we make the hypothesis that malignant cells are the main targets of these compounds since they express high levels of miR-214. In fact, even if embryos express high levels of miR-214 in most tissues, miR-214 expression is limited in adult tissues.[25] With the intent to obtain tissue specificity, an AAV8-miR-214 sponge was used to treat RIP-Tag2 mice and, similarly, tumor dissemination was also inhibited. Remarkably, no sign of toxicity has been observed for all treated mice (R97

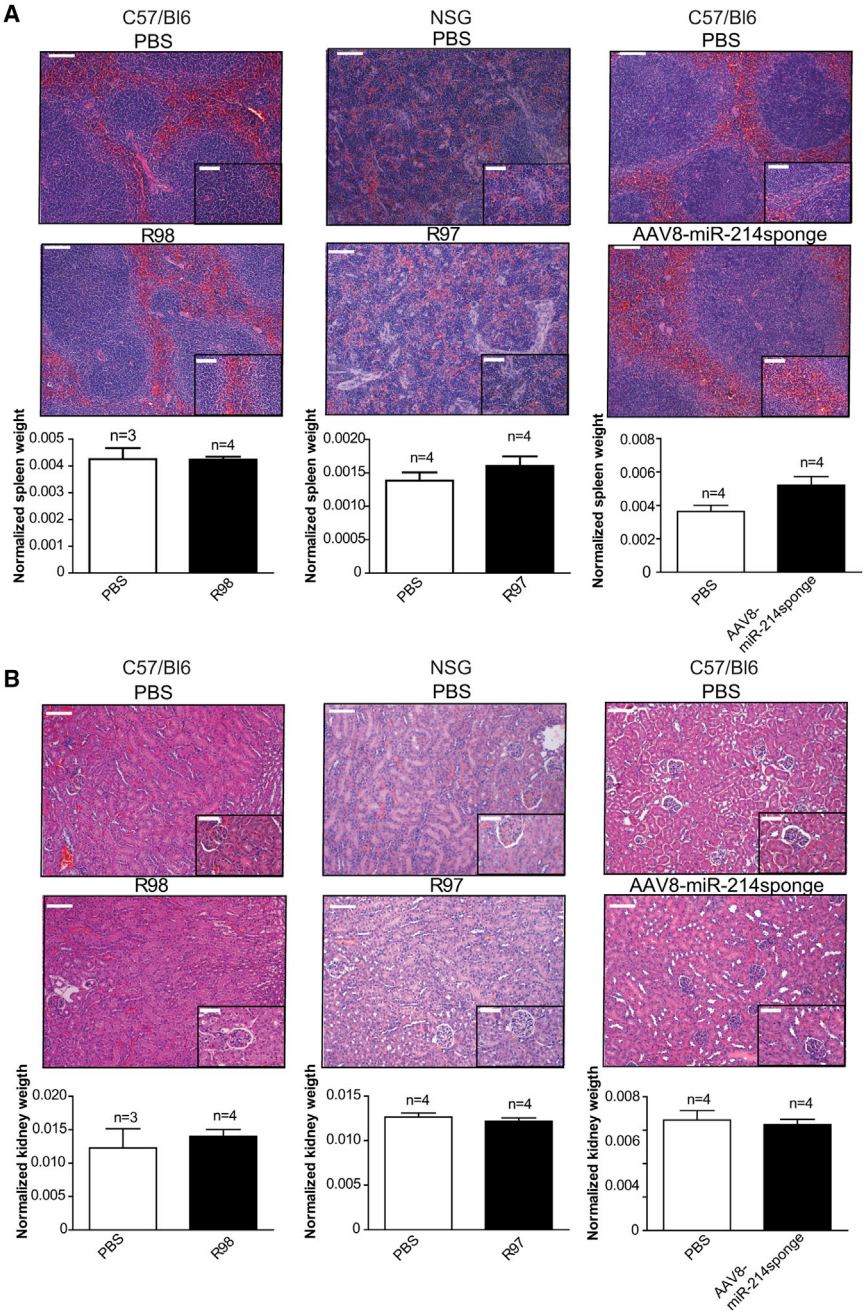

Figure 6. R97 or R98 anti-miR-214 or AAV8-miR-214 Sponge Administration Does Not Alter Spleen or Kidney Weight and Histology

(A and B) Spleen (A) and kidneys (B) of the same C57/Bl6 or NSG mice described in Figure 5 were weighted at the final time point and sections stained with H&E. Representative H&E pictures (scale bars, 100 μm) and plots corresponding to the mean ± SEM of normalized organ weight at week 4 post-treatment (organ weight versus initial mouse body weight) are shown. n, number of mice used.

or R98 anti-miR-214 or AAV8-miR-214) as shown by measuring body and organ weight or by evaluating toxicity markers. Similar results have been previously observed using anti-miR-10b in mammary tumors[26] and anti-miR-21 in glioblastomas.[27] Interestingly, in our breast tumor models miR-214 levels diminished in primary tumors, while miR-148b expression increased. As a consequence, miR-148b direct targets, *ALCAM* and *ITGA5*, were found reduced. Considering that we previously observed the involvement of the adhesion molecules ALCAM and ITGA5 in the coordination of miR-214-driven extravasation,[7,15] we can assume that R97 or R98 anti-miR-214 inhibit tumor cell dissemination by impairing extravasation in breast tumors. Nevertheless, due to the reduced number of CTCs, we can also hypothesize an effect on the detachment of cells from the primary tumor and consequent intravasation. However, considering that in melanoma tumor models we did not observe similar modulations for miR-148b and its direct targets ALCAM and ITGA5, it is possible that other mechanisms also play a role in the dissemination inhibitory functions of R97/R98 in melanoma. It is important to underline that R97/R98 or an AAV8-miR-214 sponge were also able to reduce neuroendocrine pancreatic tumor growth, which can correlate, at least in part, with the observed decrease of angiogenesis. In R97/R98-treated mice reduced proliferation was also observed, suggesting that other cell-autonomous mechanisms could be involved, besides the inhibition of angiogenesis. On the contrary, no influence on tumor growth was observed for melanomas and breast cancers. These differences on tumor growth could be linked to spontaneous neoplasias (pancreatic tumors) versus xenotransplants. Alternatively, or in combination, to the fact that RIP-Tag2 animals are immunocompetent while the immune system is impaired in mice bearing xenotransplants. However, it is also possible that the more local route of administration used for R97 or R98 anti-miR-214 oligos or an AAV8-miR-214 sponge in RIP-Tag2 animals could have been more effective compared to the systemic delivery used for xenotransplant-bearing mice. Further investigations are needed to shed light on this issue. Taking together, our results demonstrated that the interchangeable R97 or R98 anti-miR-214 oligos are powerful inhibitors of metastatic dissemination for rapidly growing tumors in mice, giving hope for a transfer to the clinics. Importantly, the application of an AAV8-miR-214 sponge to RIP-Tag2 tumors suggests that, when tumor cells can be specifically infected by a virus, unique delivery of anti-miR tools to cancer cells can be achieved.

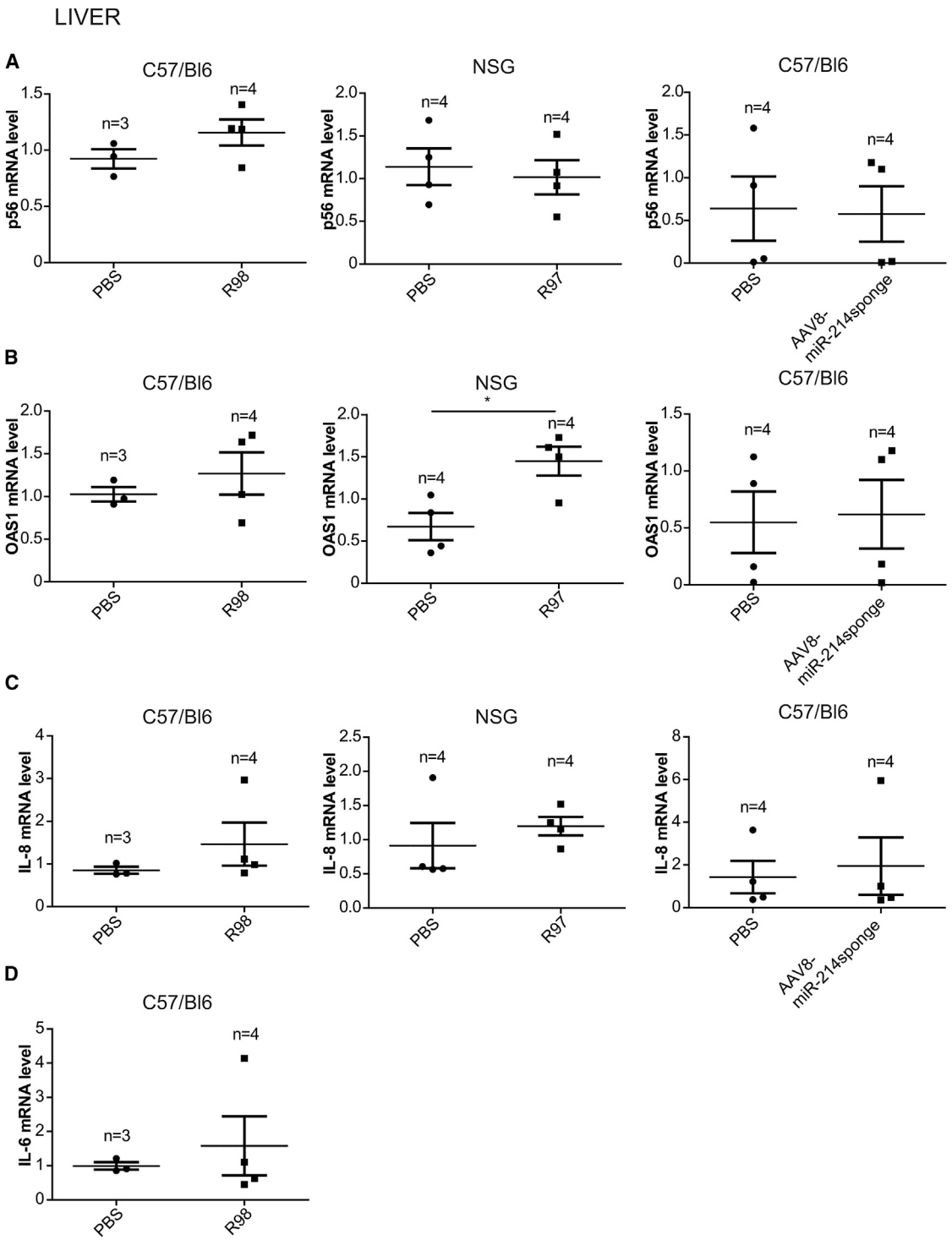

Figure 7. R97 or R98 anti-miR-214 or AAV8-miR-214 Sponge Administration Does Not Affect Toxicity Markers in the Liver of Treated Animals

(A–D) Livers of the same C57/Bl6 or NSG mice animals described in Figure 5, at the final time point (week 4 post-treatment), were used to extract total RNA and expression of *p56* (A), *OAS1* (B), *IL-8* (C), or *IL-6* (D) mRNA (toxicity genes) was measured by qRT-PCR analysis and presented as fold changes (mean ± SD of triplicates) relative to median gene expression, normalized on *18S* or *GAPDH* RNA. n, number of mice used.

MATERIALS AND METHODS

Cell Culture

MA-2 cells were kindly provided by L. Xu and R.O. Hynes[28] and maintained as described in Penna et al.;[4,7] 4175-TGL cells were a generous gift of J. Massaguè[29] and maintained in standard conditions. MA-2 miR-214over and 4175-TGL miR-214over were engineered in our lab to obtain high levels of miR-214 and tRFP expression as in Penna et al.[4] and Orso et al.[15] GFP-positive HUVECs (GFP HUVECs) were kindly provided by L. Primo and maintained as described in Penna et al.[4,7]. All used cell lines were authenticated in the last 6 months by BMR Genomics (Padova, Italy) using the CELL ID System (Promega).

Reagents

miR Inhibitors

Anti-miR miRNA Inhibitor Negative Control #1 was from Applied Biosystems (Foster City, CA), and anti-miR-214 (R97 or R98) was from Regulus Therapeutics (RT). R97 and R98 anti-miR-214 compounds are complementary to miR-214 and contain a full phosphorothioate backbone and sugar modifications, such as constrained ethyl (cEt)/DNA or fluoro/methoxyethyl at the 2′ position of the sugar. R97 and R98 are both modified along the nucleotide sequences but at diverse positions;[22] however, no biological differences were observed in our initial *in vitro* or *in vivo* experiments (see Figures 1, 2, and S1), so R97 and R98 were considered equal and used interchangeably in all experiments presented here.

TaqMan miR Assays for miRNA Detection

Hsa-miR-214 ID 002306, Hsa-miR-148b ID000471, U6 snRNA ID001973, and U44 snRNA ID001904 were from Applied Biosystems (Foster City, CA).

QuantiTect Primer Assays for Gene Detection

ITGA5 QT00080871, *ALCAM* QT00026824, and *Actin* QT00095431 were from QIAGEN (Stanford, CA). *p56* (*CDKL2*) FW, 5′-TCA AGT ATG GCA AGG CTG TG-3′, *p56* (*CDKL2*) RV, 5′-GAG GCT CTG CTT CTG CAT CT-3′; *OAS1* FW, 5′-ACC GTC TTG GAA CTG GTC AC-3′, *OAS1* RV, 5′-ATG TTC CTT GTT GGG TCA GC-3′; and *IL8* FW, 5′-GCGCCCAGACAGAAGTCATAG-3′, *IL8* RV, 5′-GGCAAACTTTTTGACCGCC-3′ were from Eurofins Genomics. *IL6* FW, 5′-GCTACCAAACTGGATATAATCAGGA-3′, *IL6* RV, 5′-CCAGGTAGCTATGGTACTCCAGAA-3′, Probe #6 was from Roche, Universal Probe Library.

Transfections

To obtain transient anti-miR expression, cells were treated as in Penna et al.[4] 0.1 or 5 μM R97 or R98 anti-miR-214 or anti-ctl were used.

RNA Isolation and qRT-PCRs

Total RNA extracts and qRT-PCR analyses were performed from cells or tumors as described in Penna et al.[4,7] and Raimo et al.[30] For RNA isolation from frozen tissues, 10 sections of 30 μm were cut from OCT embedded samples and homogenized in Trizol (Thermofisher Scientific) using a tissue homogenizer (Qiagen). Samples were than centrifuged for 10 minutes at 14,000 rpm, supernatants were transferred to fresh tubes, and RNA extraction was performed according to the manufacturer's instructions.

Adeno-associated Vector Preparations and Viral Production

The AAV8-miR-214 sponge construct was generated according to Maione et al.,[31] starting from the pAAV-MCS vector from Stratagene (Agilent Technologies, CA) in which the miR-214 sponge sequence[4] was inserted. The viral stocks were obtained using a packaging plasmid encoding the serotype 8 capsid protein;[31] titer, 1×10^{12} to 1×10^{13} viral genome particles/mL.

In Vitro Migration and Transendothelial Migration and *In Vivo* Extravasation Assays

In vitro migration, transendothelial migration, and *in vivo* extravasation assays were performed as in Penna et al.[4]

In Vivo Tumor Growth and Metastatic Dissemination

All experiments performed with live animals complied with ethical care and were approved by the Animal Care Committee of the Molecular Biotechnology Center and the Italian Ministry of Health. For tumor growth and experimental metastasis assays, 4175-TGL-pLemiR-214 or MA-2-pLemiR-214 cells (in PBS) were injected in mice as in Penna et al.[7] Primary tumors, lung metastasis, or nodule formation were evaluated as in Raimo et al.[30]

CTCs

Blood was collected from the right atrium by heart puncture with a 25G needle syringe containing 0.1 mL of heparin. Blood was plated in tissue culture medium, and 3 days later tumor cells were selected with puromycin, and then colonies or total number of cells were counted.

RIP-Tag2 Mouse Model and *In Vivo* AAV8-miR-214 Sponge Administration

All experiments performed were approved by the Animal Care Committee of the Candiolo Cancer Institute and the Italian Ministry of Health. The RIP-Tag2 transgenic mouse model has been previously described.[31] In brief, RIP-Tag2 transgenic mice express the oncogenic SV40 large TAg under the transcriptional control of the rat insulin promoter and the entire course of tumor development can be closely followed. In fact, RIP-Tag2 mice develop hyperplastic and dysplastic islets that eventually become angiogenic, form invasive carcinomas, and metastasize. From 12 weeks of age, when the angiogenic switch of the pancreatic islets occurs, all mice received 50% sugar food (Harlan Teklad) and 5% sugar water to relieve hypoglycemia induced by the insulin-secreting altered islets. At week 12, mice were injected (one time only) in the pancreas, through the superior mesenteric artery, with a PBS solution of AAV8-miR-214 sponge or PBS only and sacrificed at week 16, if mice did not die before, as previously detailed.[31]

Anti-miR-214 Administration to Mice

10 mg/kg of animal weight (equal to 0.25 mg/mouse) of R97 or R98 anti-miR-214 (Regulus Therapeutics, San Diego, CA, USA) dissolved in PBS or PBS only (control) were administered (tail vein) to age- and gender-matched NSG mice (day 2) injected 2 days before (day 1) with tumor cells (tail vein) and every other day until sacrifice. Alternatively, mice were injected subcutaneously or into the fat pad (day 0) with MA-2 or 4175-TGL cells, respectively, and treated similarly from day 2. The same compounds were also administered intraperitoneally to RIP-Tag2 mice twice a week for 1 month (from week 12 to week 16 of age).

Evaluation of Peripancreatic Lymph Node Metastasis

In RIP-Tag2 transgenic mice, the presence or absence of tumor cell dissemination was evaluated in the peripancreatic LNs at week 16, or before if mice did not survive until then. Peripancreatic LNs from each treatment group were collected at sacrifice and embedded in optimal cutting temperature (OCT) compound, then cut into serial sections. The presence or absence of tumor metastasis was evaluated by immunostaining using a rabbit anti-SV40 TAg antibody (catalog #sc-20800, 1:50; Santa Cruz). Fluorescent confocal microscopy images were quantified with ImageJ software. In each image, we drew a line corresponding to the width (w) of the metastatic region and a line corresponding to the length (l), and we calculated the LN metastasis volume according to the spheroid volume formula: $0.52 \times w^2 \times l$.

Evaluation of Proliferation, Apoptosis and Vessel Area in RIP-Tag2 Pancreatic Neuroendocrine Tumors

OCT-embedded frozen samples were cut into 5-μm-thick sections. Slides were incubated with the following primary antibodies: rabbit monoclonal anti-ki67 (Thermo Fisher Scientific; 1:100), rabbit monoclonal anti-cleaved caspase 3 (asp175, clone 5A1, Cell Signaling; 1:50), or rat monoclonal anti-panendothelial cell antigen anti-MECA32 (550563, BD Pharmingen; 1:100), overnight at 4°C in a moist chamber. After rinsing in PBS, Alexa Fluor secondary antibodies were added. DAPI was used to counterstain the nuclei (Thermo Fisher). The slides were analyzed under a Leica DM IRBM microscope. To determine the expression levels of Ki67 or cleaved caspase 3 in each analyzed image, the mean fluorescence intensity (MFI) of red channel was measured and the values normalized by comparing stained area with the total cells (DAPI) present in the tissue area. Tumor vessel area was quantified as the area occupied by Meca32-positive structures, compared with the total tissue area visualized by DAPI. ImageJ software was used for image analysis.

Toxicity Evaluation for R97 or R98 Anti-miR-214 Compounds or for the AAV8-miR-214 Sponges *In Vivo*

Toxicity for R97 or R98 anti-miR-214 oligos or AAV8-miR-214 sponges was evaluated *in vivo* by measuring body and organ (liver, spleen, kidneys) weight of treated versus untreated (PBS) animals during the course of the experiment or at the final point, as in Maione et al.[32] In addition, total RNA was extracted from liver, spleen, and kidneys of treated and control (PBS-treated) animals and expression of toxicity genes (*p56*, *OAS1*, *IL-6*, or *IL-8*) was studied by qRT-PCR analysis as in Esposito et al.[23] The same organs were also used to perform tissue histology analysis following H&E staining as in Orso et al.[15]

Statistical Analysis

The results are shown as mean ± SD or ± SEM, as indicated, and the two-tailed Student's t test was used for comparison. *$p < 0.05$; **$p < 0.01$; ***$p < 0.001$ were considered to be statistically significant.

SUPPLEMENTAL INFORMATION

Supplemental Information includes five figures and can be found with this article online at https://doi.org/10.1016/j.ymthe.2018.05.020.

AUTHOR CONTRIBUTIONS

Conception, Design, and Supervision, D.T.; Development and Methodology, F.O., E.P., D.D., D.B., S.B., E.T., F.M..; Data Acquisition, Analysis, and Interpretation, F.O., E.P., D.D., F.M., E.G.; Anti-miR-214 Development and Testing, Regulus Therapeutics; Writing the Manuscript, D.T.

CONFLICTS OF INTEREST

The authors declare no competing financial interests.

ACKNOWLEDGMENTS

D.T. was supported by Compagnia di San Paolo, Torino (2008.1054), AIRC 2010, 2013, 2017 (IG2010-10104, IG2013-14201, and IG2017-20258), Fondazione Cassa di Risparmio Torino CRT (2014.1085), and Progetto di ricerca di Ateneo 2017/SanPaolo Torino CST0165134. F.O. was supported by the FIRB giovani 2008 project (RBFR08F2FS-002). E.P. was supported by a FIRC fellowship (2012–2014). D.D. is a Veronesi Fellow (2016–2017). E.G.was supported by AIRC (AIRC-IG grant 15645), the Swiss National Science Foundation (SNSF), a Sinergia grant (CRSII3 160742/1), and a FPRC-ONLUS grant—"5 per mille 2014 Ministero Salute. We are grateful to Lei Xu and Richard Hynes for the MA-2 cell line; Joan Massagué for the 4175-TGL cells; Luca Primo for the GFP-HUVECs; Flavio Cristofani for his help with the immunocompromised mice; Marco Forni for pictures of histological sections; Sofia Bertone for technical help and Guido Tarone (deceased), Fiorella Balzac, and Cristina Rubinetto for their help with the AAV8-miR-214 sponge. We thank Regulus Therapeutics Inc. for R97 and R98 compounds. We are profoundly grateful to Dimitrios G. Zisoulis for his essential contribution to this project and his continuous scientific support in the early settings of R97- and R98-related experiments and during the revision stage.

REFERENCES

1. Gupta, G.P., and Massagué, J. (2006). Cancer metastasis: building a framework. Cell *127*, 679–695.

2. Parkin, D.M., Bray, F., Ferlay, J., and Pisani, P. (2005). Global cancer statistics, 2002. CA Cancer J. Clin. *55*, 74–108.

3. Chen, Y., Gao, D.Y., and Huang, L. (2015). In vivo delivery of miRNAs for cancer therapy: challenges and strategies. Adv. Drug Deliv. Rev. *81*, 128–141.

4. Penna, E., Orso, F., Cimino, D., Tenaglia, E., Lembo, A., Quaglino, E., Poliseno, L., Haimovic, A., Osella-Abate, S., De Pittà, C., et al. (2011). microRNA-214 contributes to melanoma tumour progression through suppression of TFAP2C. EMBO J. *30*, 1990–2007.

5. Olson, P., Lu, J., Zhang, H., Shai, A., Chun, M.G., Wang, Y., Libutti, S.K., Nakakura, E.K., Golub, T.R., and Hanahan, D. (2009). MicroRNA dynamics in the stages of tumorigenesis correlate with hallmark capabilities of cancer. Genes Dev. *23*, 2152–2165.

6. Zhang, X.J., Ye, H., Zeng, C.W., He, B., Zhang, H., and Chen, Y.Q. (2010). Dysregulation of miR-15a and miR-214 in human pancreatic cancer. J. Hematol. Oncol. *3*, 46.

7. Penna, E., Orso, F., Cimino, D., Vercellino, I., Grassi, E., Quaglino, E., Turco, E., and Taverna, D. (2013). miR-214 coordinates melanoma progression by upregulating ALCAM through TFAP2 and miR-148b downmodulation. Cancer Res. *73*, 4098–4111.

8. Molnár, V., Tamási, V., Bakos, B., Wiener, Z., and Falus, A. (2008). Changes in miRNA expression in solid tumors: an miRNA profiling in melanomas. Semin. Cancer Biol. *18*, 111–122.

9. Segura, M.F., Belitskaya-Lévy, I., Rose, A.E., Zakrzewski, J., Gaziel, A., Hanniford, D., Darvishian, F., Berman, R.S., Shapiro, R.L., Pavlick, A.C., et al. (2010). Melanoma microRNA signature predicts post-recurrence survival. Clin. Cancer Res. *16*, 1577–1586.

10. Worley, L.A., Long, M.D., Onken, M.D., and Harbour, J.W. (2008). Micro-RNAs associated with metastasis in uveal melanoma identified by multiplexed microarray profiling. Melanoma Res. *18*, 184–190.

11. Zhang, L., Huang, J., Yang, N., Greshock, J., Megraw, M.S., Giannakakis, A., Liang, S., Naylor, T.L., Barchetti, A., Ward, M.R., et al. (2006). microRNAs exhibit high frequency genomic alterations in human cancer. Proc. Natl. Acad. Sci. USA *103*, 9136–9141.

12. Sempere, L.F., Christensen, M., Silahtaroglu, A., Bak, M., Heath, C.V., Schwartz, G., Wells, W., Kauppinen, S., and Cole, C.N. (2007). Altered microRNA expression confined to specific epithelial cell subpopulations in breast cancer. Cancer Res. *67*, 11612–11620.

13. Ali, S., Dubaybo, H., Brand, R.E., and Sarkar, F.H. (2015). Differential expression of microRNAs in tissues and plasma co-exists as a biomarker for pancreatic cancer. J. Cancer Sci. Ther. *7*, 336–346.

14. Blenkiron, C., Goldstein, L.D., Thorne, N.P., Spiteri, I., Chin, S.F., Dunning, M.J., Barbosa-Morais, N.L., Teschendorff, A.E., Green, A.R., Ellis, I.O., et al. (2007). MicroRNA expression profiling of human breast cancer identifies new markers of tumor subtype. Genome Biol. *8*, R214.

15. Orso, F., Quirico, L., Virga, F., Penna, E., Dettori, D., Cimino, D., Coppo, R., Grassi, E., Elia, A.R., Brusa, D., et al. (2016). miR-214 and miR-148b targeting inhibits dissemination of melanoma and breast cancer. Cancer Res. *76*, 5151–5162.

16. Henry, J.C., Azevedo-Pouly, A.C., and Schmittgen, T.D. (2011). MicroRNA replacement therapy for cancer. Pharm. Res. *28*, 3030–3042.

17. Rupaimoole, R., and Slack, F.J. (2017). MicroRNA therapeutics: towards a new era for the management of cancer and other diseases. Nat. Rev. Drug Discov. *16*, 203–222.

18. Crooke, S.T., Vickers, T., Lima, W.F., and Wu, H. (2007). Mechanisms of antisense drug action, an introduction. In Antisense Drug Technology: Principles, Strategies and Applications, S.T. Crooke, ed. (CRC Press), pp. 3–46.

19. van der Ree, M.H., de Vree, J.M., Stelma, F., Willemse, S., van der Valk, M., Rietdijk, S., Molenkamp, R., Schinkel, J., van Nuenen, A.C., Beuers, U., et al. (2017). Safety, tolerability, and antiviral effect of RG-101 in patients with chronic hepatitis C: a phase 1B, double-blind, randomised controlled trial. Lancet *389*, 709–717.

20. Chau, B.N., Xin, C., Hartner, J., Ren, S., Castano, A.P., Linn, G., Li, J., Tran, P.T., Kaimal, V., Huang, X., et al. (2012). MicroRNA-21 promotes fibrosis of the kidney by silencing metabolic pathways. Sci. Transl. Med. *4*, 121ra18.

21. Gomez, I.G., MacKenna, D.A., Johnson, B.G., Kaimal, V., Roach, A.M., Ren, S., Nakagawa, N., Xin, C., Newitt, R., Pandya, S., et al. (2015). Anti-microRNA-21 oligonucleotides prevent Alport nephropathy progression by stimulating metabolic pathways. J. Clin. Invest. *125*, 141–156.

22. Hogan, D.J., Vincent, T.M., Fish, S., Marcusson, E.G., Bhat, B., Chau, B.N., and Zisoulis, D.G. (2014). Anti-miRs competitively inhibit microRNAs in Argonaute complexes. PLoS ONE *9*, e100951.

23. Esposito, C.L., Cerchia, L., Catuogno, S., De Vita, G., Dassie, J.P., Santamaria, G., Swiderski, P., Condorelli, G., Giangrande, P.H., and de Franciscis, V. (2014). Multifunctional aptamer-miRNA conjugates for targeted cancer therapy. Mol. Ther. *22*, 1151–1163.

24. Geary, R.S., Norris, D., Yu, R., and Bennett, C.F. (2015). Pharmacokinetics, biodistribution and cell uptake of antisense oligonucleotides. Adv. Drug Deliv. Rev. *87*, 46–51.

25. Watanabe, T., Sato, T., Amano, T., Kawamura, Y., Kawamura, N., Kawaguchi, H., Yamashita, N., Kurihara, H., and Nakaoka, T. (2008). Dnm3os, a non-coding RNA, is required for normal growth and skeletal development in mice. Dev. Dyn. *237*, 3738–3748.

26. Ma, L., Reinhardt, F., Pan, E., Soutschek, J., Bhat, B., Marcusson, E.G., Teruya-Feldstein, J., Bell, G.W., and Weinberg, R.A. (2010). Therapeutic silencing of miR-10b inhibits metastasis in a mouse mammary tumor model. Nat. Biotechnol. *28*, 341–347.

27. Lee, T.J., Yoo, J.Y., Shu, D., Li, H., Zhang, J., Yu, J.G., Jaime-Ramirez, A.C., Acunzo, M., Romano, G., Cui, R., et al. (2017). RNA nanoparticle-based targeted therapy for glioblastoma through inhibition of oncogenic miR-21. Mol. Ther. *25*, 1544–1555.

28. Xu, L., Shen, S.S., Hoshida, Y., Subramanian, A., Ross, K., Brunet, J.P., Wagner, S.N., Ramaswamy, S., Mesirov, J.P., and Hynes, R.O. (2008). Gene expression changes in an animal melanoma model correlate with aggressiveness of human melanoma metastases. Mol. Cancer Res. *6*, 760–769.

29. Minn, A.J., Gupta, G.P., Siegel, P.M., Bos, P.D., Shu, W., Giri, D.D., Viale, A., Olshen, A.B., Gerald, W.L., and Massagué, J. (2005). Genes that mediate breast cancer metastasis to lung. Nature *436*, 518–524.

30. Raimo, M., Orso, F., Grassi, E., Cimino, D., Penna, E., De Pittà, C., Stadler, M.B., Primo, L., Calautti, E., Quaglino, P., et al. (2016). miR-146a exerts differential effects on melanoma growth and metastatization. Mol. Cancer Res. *14*, 548–562.

31. Maione, F., Molla, F., Meda, C., Latini, R., Zentilin, L., Giacca, M., Seano, G., Serini, G., Bussolino, F., and Giraudo, E. (2009). Semaphorin 3A is an endogenous angiogenesis inhibitor that blocks tumor growth and normalizes tumor vasculature in transgenic mouse models. J. Clin. Invest. *119*, 3356–3372.

32. Maione, F., Oliaro-Bosso, S., Meda, C., Di Nicolantonio, F., Bussolino, F., Balliano, G., Viola, F., and Giraudo, E. (2015). The cholesterol biosynthesis enzyme oxidosqualene cyclase is a new target to impair tumour angiogenesis and metastasis dissemination. Sci. Rep. *5*, 9054.